Published in final edited form as:
Mol Microbiol. 2010 April ; 76(1): 159–172. doi:10.1111/j.1365-2958.2010.07089.x.

The Differential Affinity of the Usher for Chaperone-Subunit Complexes is Required for Assembly of Complete Pili

Qinyuan Li[1], **Tony W. Ng**[1,†], **Karen W. Dodson**[2], **Stephane Shu Kin So**[1,¶], **Ken-Michael Bayle**[1,‡], **Jerome S. Pinkner**[2], **Suzanne Scarlata**[3], **Scott J. Hultgren**[2], and **David G. Thanassi**[1,*]

[1] Center for Infectious Diseases, Department of Molecular Genetics and Microbiology, Stony Brook University, Stony Brook, NY 11794-5120, USA

[2] Department of Molecular Microbiology, Washington University School of Medicine, St. Louis, MO 63110, USA

[3] Department of Physiology and Biophysics, Stony Brook University, Stony Brook, NY 11794-8661, USA

SUMMARY

Attachment to host cells via adhesive surface structures is a prerequisite for the pathogenesis of many bacteria. Uropathogenic *E. coli* assemble P and type 1 pili for attachment to the host urothelium. Assembly of these pili requires the conserved chaperone/usher pathway, in which a periplasmic chaperone controls the folding of pilus subunits and an outer membrane usher provides a platform for pilus assembly and secretion. The usher has differential affinity for pilus subunits, with highest affinity for the tip-localized adhesin. Here, we identify residues F21 and R652 of the P pilus usher PapC as functioning in the differential affinity of the usher. R652 is important for high affinity binding to the adhesin whereas F21 is important for limiting affinity for the PapA major rod subunit. PapC mutants in these residues are specifically defective for pilus assembly in the presence of PapA, demonstrating that differential affinity of the usher is required for assembly of complete pili. Analysis of PapG deletion mutants demonstrated that the adhesin is not required to initiate P pilus biogenesis. Thus, the differential affinity of the usher may be critical to ensure assembly of functional pilus fibers.

Keywords

bacteria; pili; fimbriae; usher; chaperone; protein secretion

INTRODUCTION

Pathogenic bacteria assemble adhesive surface structures to bind to host cells and initiate the infectious process. Uropathogenic *Escherichia coli* (UPEC), which is the most common causative agent of urinary tract infections (Foxman and Brown, 2003), use adhesive, hair-like fibers termed pili (fimbriae) to colonize the urinary tract. UPEC express P pili to bind receptors in the kidney, leading to the development of pyelonephritis, and type 1 pili to attach to receptors in the bladder, initiating a cascade of events leading to the development

[*]Correspondence to: David.Thanassi@stonybrook.edu; Phone, 631-632-454; Fax, 631-632-4294.
[†]Present Address: Department of Microbiology and Immunology, Albert Einstein College of Medicine, Bronx, NY 10461, USA
[¶]Present Address: Massachusetts Institute of Technology, Sloan School of Management, Cambridge, MA 02142, USA
[‡]Present Address: New York College of Osteopathic Medicine of New York Institute of Technology, Old Westbury, New York 11568, USA

of cystitis (Roberts *et al.*, 1994; Wright *et al.*, 2007). P and type 1 pili are prototype fibers assembled by the chaperone/usher (CU) secretion pathway, which is used by many Gram-negative bacteria for the assembly of virulence-associated surface structures (Sauer *et al.*, 2004).

P pili are encoded by the chromosomal *pap* gene cluster. P pili consist of six structural proteins that connect end-to-end to form a fiber composed of two distinct sub-assemblies: a 8.2 nm thick rigid helical rod and a 2 nm diameter flexible tip that is located at the distal end of the rod (Fig. 1) (Kuehn *et al.*, 1992;Mu and Bullitt, 2006). The rod contains over 1,000 copies of the PapA major pilus subunit and is terminated by the PapH subunit, which may also help anchor the pilus in the bacterial outer membrane (OM) (Baga *et al.*, 1987;Verger *et al.*, 2006). The P pilus tip contains several copies of the PapE subunit and is linked to the rod via the PapK adaptor subunit. The PapG adhesin is present in single copy at the distal end of the tip and confers binding to Galα(1-4)Gal moieties present in kidney glycolipids (Lund *et al.*, 1987). PapG is linked to PapE via the PapF adaptor subunit (Fig. 1).

Pilus assembly by the CU pathway requires two specialized assembly factors known as the periplasmic chaperone (PapD for P pili) and OM usher (PapC for P pili). Following translocation across the cytoplasmic membrane via the Sec general secretory pathway (Driessen and Nouwen, 2008), P pilus subunits must interact with the PapD chaperone for proper folding and stabilization (Fig. 1). Pilus subunits contain an incomplete immunoglobulin (Ig)-like fold termed the pilin domain. The chaperone facilitates the folding of pilus subunits by donating a β-strand to complete the subunit pilin domain, in a mechanism termed donor strand complementation (Choudhury *et al.*, 1999; Sauer *et al.*, 1999). Periplasmic chaperone-subunit complexes next must interact with the OM usher. The usher catalyzes subunit assembly into the pilus fiber and provides the channel for secretion of the fiber to the cell surface (Fig. 1) (Norgren *et al.*, 1987; Nishiyama *et al.*, 2008; Remaut *et al.*, 2008). All pilus subunits except the adhesin contain a conserved N-terminal extension (Nte) in addition to the pilin domain (Fig. 1). Subunit-subunit interactions form at the usher when the Nte from an incoming chaperone-subunit complex displaces the donated chaperone β-strand from the preceding chaperone-subunit complex, completing the Ig fold of the preceding subunit in a mechanism termed donor strand exchange (Sauer *et al.*, 2002; Zavialov *et al.*, 2003). Thus, the pilus fiber is built from an array of Ig folds, with each subunit bound to the preceding subunit by donor strand exchange (Fig. 1). The adhesin, which is located at the tip of the pilus, contains an N-terminal adhesin domain in place of the Nte. Donor strand exchange allows subunits to adopt a lower energy state compared to donor strand complementation with the chaperone; the exchange of chaperone-subunit for subunit-subunit interactions is thought to energize pilus biogenesis at the usher (Sauer *et al.*, 2002; Zavialov *et al.*, 2005).

The PapC usher is an integral OM protein containing 809 amino acids. The usher contains four distinct domains: a transmembrane β-barrel domain, a middle or plug domain that interrupts the β–barrel domain, and periplasmic N- and C-terminal domains (Fig. 1) (Nishiyama *et al.*, 2005;Shu Kin So and Thanassi, 2006;Remaut *et al.*, 2008). The β-barrel domain forms the translocation channel, which is large enough to allow secretion of a linear fiber of folded pilus subunits (Remaut *et al.*, 2008). In the resting usher, the translocation channel is gated shut by the internal plug domain (Fig. 1) (Remaut *et al.*, 2008;Mapingire *et al.*, 2009). The N-terminal domain (residues 1-125) provides the initial binding site for periplasmic chaperone-subunit complexes (Ng *et al.*, 2004;Nishiyama *et al.*, 2005), whereas the C-terminal domain (residues 641-809) is required for subsequent pilus assembly events (Thanassi *et al.*, 2002;Shu Kin So and Thanassi, 2006). The usher functions in the OM as a dimeric complex, but only one channel is used for secretion of the pilus fiber (Li *et al.*, 2004;Shu Kin So and Thanassi, 2006;Remaut *et al.*, 2008). The usher dimer may be required

for successive rounds of recruitment of chaperone-subunit complexes from the periplasm and to position subunits for donor strand exchange (Remaut *et al.*, 2008;Li and Thanassi, 2009).

Pili are assembled in a defined order, with the adhesin incorporated first, followed by the rest of the tip and finally the rod. Each subunit specifically interacts with its appropriate neighbor subunit in the pilus, with the specificity of binding determined by the donor strand exchange reaction (Lee *et al.*, 2007; Rose *et al.*, 2008). In addition, the usher differentially recognizes chaperone-subunit complexes according to their final position in the pilus (Dodson *et al.*, 1993; Saulino *et al.*, 1998). Thus, the chaperone-adhesin complex binds to the usher with both highest affinity and fastest association rate compared to other chaperone-subunit complexes (Saulino *et al.*, 1998). This differential affinity of the usher is thought to ensure that the adhesin is the first subunit incorporated into the pilus. However, the role of the differential affinity of the usher in pilus assembly has not been defined and the mechanism whereby the usher discriminates among chaperone-subunit complexes is not known. Previous studies showed that the usher N-terminal domain directly binds chaperone-subunit complexes (Ng *et al.*, 2004; Nishiyama *et al.*, 2005) and the isolated N-terminal domain of the type 1 pilus usher FimD retains differential affinity for chaperone-subunit complexes (Nishiyama *et al.*, 2003). Thus, the N-terminal domain clearly participates in discrimination among chaperone-subunit complexes. The usher C-terminal domain is also important for interactions with chaperone-subunit complexes and the isolated PapC C-terminal domain was shown to directly bind PapDG chaperone-adhesin complexes (Shu Kin So and Thanassi, 2006). This suggests that the C-terminal domain may also participate in the differential affinity of the usher.

In this study, we investigated the mechanism of the N- and C-terminal domains in the differential affinity of the usher for chaperone-subunit complexes. We show that both domains of PapC are important for discrimination among chaperone-subunit complexes and that differential affinity is required for assembly of complete pili. Furthermore, we show that the PapG adhesin is not required to initiate assembly of P pili on the bacterial surface. Thus, the differential affinity of the usher for the adhesin may be particularly important for P pilus biogenesis to ensure assembly of adhesive organelles.

RESULTS AND DISCUSSION

A PapC F21A mutant is defective for pilus assembly, but able to assemble pilus tips in the absence of PapA

The usher N-terminal domain provides the initial binding site for chaperone-subunit complexes (Ng *et al.*, 2004; Nishiyama *et al.*, 2005). A co-crystal structure of the FimD N-terminal domain bound to a FimC chaperone-FimH pilin domain complex revealed that the first 24 residues of FimD specifically interact with the bound complex and that three phenylalanines within this region (F4, F8 and F22) make direct contacts (Nishiyama *et al.*, 2005). Mutation of these residues to alanine rendered FimD partly (F8A) or completely (F4A and F22A) unable to assemble type 1 pili, and the F4A and F8A mutations prevented the FimD N-terminal domain from binding chaperone-subunit complexes in vitro (Nishiyama *et al.*, 2005). Within the PapC N-terminal domain, residues F3 and F21 are conserved with FimD residues F4 and F22, respectively (Fig. 2A). PapC does not have a phenylalanine corresponding to FimD F8, but contains an additional phenylalanine at position 18 (Fig. 2A). In agreement with the FimD data, we previously demonstrated that PapC residues 2-11 are required for the usher to bind chaperone-subunit complexes and assemble pili, and that PapC F3 is a critical residue within this region (Ng *et al.*, 2004; Ng *et al.*, 2006). To determine if PapC F18 and F21 might be similarly important for pilus biogenesis, we constructed alanine substitution mutations of these residues. The PapC F18A

and F21A mutants were expressed at similar levels in the OM compared to WT PapC (see upper panel in Fig. 3A) and the mutations did not affect folding of the ushers, as assessed by resistance to denaturation by SDS (data not shown).

A hemagglutination assay was performed to test the ability of the PapC F18A and F21A mutants to complement a Δ*papC pap* operon (*papAHDJKEFG*) for assembly of adhesive P pili on the bacterial surface. As shown in Table 1, whereas bacteria expressing PapC F18A showed only a slight decrease in agglutination of human red blood cells compared to WT PapC, the F21A mutant had no agglutination activity, identical to the vector and PapC Δ2-11 negative controls. Purification of pili from the bacterial surface by heat extraction and magnesium precipitation confirmed that the hemagglutination defect of PapC F21A was due to a loss of pilus assembly (Fig. 2B). In contrast, the F18A mutant assembled pili similar to WT PapC, although at a reduced level in accordance with the hemagglutination results. These data demonstrate that residue F21, but not F18, is critical for pilus assembly by PapC.

To probe the basis for the pilus assembly defect of the PapC F21A mutant, we examined its ability to bind PapDG chaperone-adhesin complexes using an in vitro overlay assay. Interestingly, the F21A mutant retained ability to bind PapDG, although the amount of protein bound was reduced compared to WT PapC and the F18A mutant (Fig. 3A). In contrast, PapC Δ2-11 and the vector control were unable to bind PapDG (Fig. 3A), as shown previously (Ng *et al.*, 2004). To confirm the in vitro overlay results, we expressed the PapC F21A mutant together with pilus tip subunits (*papDJKEFG*) and analyzed the ability of the usher to co-purify with the pilus subunits from bacteria. As shown in Fig. 3B, pilus tip subunits co-purified with PapC F21A similar to WT PapC and PapC F18A, although at reduced levels. This was in contrast to PapC Δ2-11 and the vector control, for which tip subunits did not co-purify. Thus, the PapC F21A mutant is able to form stable interactions with chaperone-subunit complexes both in vivo and in vitro. These data indicate that the function of residue F21 of PapC is distinct from the role of the usher N-terminal domain in binding chaperone-subunit complexes.

Since PapC F21A was able to bind pilus tip subunits in vivo, we asked whether this mutant was capable of assembling functional P pilus tips on the bacterial surface, using the hemagglutination assay. When co-expressed in bacteria with pilus tip subunits (*papDJKEFG*), the F21A mutant showed only a slight decrease in agglutination of human red blood cells compared to WT PapC and the F18A mutant (Table 1), indicating that PapC F21A is functional in bacteria for assembly of pilus tips. Therefore, although PapC F21A was unable to assemble pili on the bacterial surface when used to complement the complete *pap* operon (Table 1 and Fig. 2B), this mutant was essentially fully functional for assembling pilus tips when the PapA rod subunit was absent. Note that when PapA was present, no pilus structures were assembled; pilus rods were not assembled, since pili could not be purified from the bacterial surface, and pilus tips were not assembled, since exposure of PapG on the bacterial surface would have resulted in hemagglutination activity.

PapC F21A and R652A mutants are specifically defective for pilus assembly in the presence of the PapA rod subunit

The phenotype of the F21A mutation in the PapC N-terminal domain closely matches the phenotype previously determined for a R652A mutation in the usher C-terminal domain (Shu Kin So and Thanassi, 2006). PapC R652A was also defective for pilus biogenesis, but able to bind chaperone-subunit complexes and assemble functional P pilus tips in the absence of PapA. A possible explanation for the phenotypes of the PapC F21A and R652A mutants is that residues F21 and R652 are important for the differential affinity of the usher for chaperone-subunit complexes. The *papA* gene is expressed at a higher level compared to the other *pap* genes and PapDA complexes are present at higher concentration in the

periplasm relative to the other chaperone-subunit complexes (Baga *et al.*, 1987; Baga *et al.*, 1988). Despite this, PapDG binds first to the usher to initiate pilus biogenesis, presumably due to its higher affinity for the usher (Dodson *et al.*, 1993; Saulino *et al.*, 1998). Therefore, if the PapC F21A and R652A mutations weaken affinity of the usher for PapDG and/or enhance affinity for PapDA, this might allow the high concentrations of PapA in the periplasm to outcompete PapG and the other pilus tip subunits for binding to PapC, blocking initiation of pilus assembly. In the absence of PapA, assembly of pilus tip fibers would proceed normally, as the tip subunits are present at similar concentrations.

To test this model, we constructed strains harboring PapDA complexes under control of an arabinose-inducible promoter, and the PapC usher and pilus tip subunits under control of IPTG-inducible promoters. In the presence of IPTG and absence of arabinose, only pilus tips will be assembled on the bacterial surface. Addition of increasing amounts of arabinose can then be used to titrate expression of PapDA and shift from assembly of pilus tips to assembly of complete pili. Analysis of periplasm fractions from these strains confirmed the expected response of PapDA protein levels to addition of arabinose (data not shown). Using this experimental system, we found no changes in hemagglutination titer upon addition of arabinose for bacteria expressing WT PapC (Table 2). In contrast, for bacteria expressing the PapC F21A or R652A mutants, addition of increasing amounts of arabinose led to a corresponding decrease in hemagglutination titer (Table 2). Purification of pili from the bacterial surface confirmed that the hemagglutination titers reflected the assembly of pili on the bacterial surface; i.e., WT PapC assembled complete pili upon addition of arabinose, but only low levels of pili could be purified from the mutants (data not shown). These data show that the PapC mutants are sensitive to PapDA expression levels, and provide support for our proposed model that residues F21 and R652 are important for the ability of the usher to discriminate among chaperone-subunit complexes and initiate pilus assembly in the face of high PapDA concentrations in the periplasm.

The PapC F21A and R652A mutants have altered binding affinities for PapDG and PapDA chaperone-subunit complexes

To quantitatively measure the effects of the F21A and R652A mutations on the binding affinity of PapC for chaperone-subunit complexes, we developed an in vitro, fluorescence-based assay using purified proteins. We first tested binding of PapDG chaperone-adhesin complexes to the PapC usher. Purified PapDG was labeled with the amine-reactive fluorescent probe coumarin SE. Coumarin is sensitive to the polarity of its surroundings and, in general, its intensity will vary greatly when it is transferred from a water to a protein environment. This property allowed us to monitor the association of purified PapC to coumarin-labeled PapDG by measuring the change in the integrated intensity of coumarin-PapDG fluorescence as PapC was incrementally added. Using this assay, we calculated an apparent equilibrium bimolecular dissociation constant (K_d) of 59 nM for PapDG binding to WT PapC (Fig. 4A). This value agrees well with the K_d of 90 nM determined previously by surface plasmon resonance (Saulino *et al.*, 1998). As a control for the specificity of the assay, we did not detect binding of the PapD chaperone alone to PapC (data not shown). The chaperone alone was previously shown not to interact with the usher (Dodson *et al.*, 1993;Saulino *et al.*, 1998). As a second control, we did not detect binding of PapDG to the PapC Δ2-11 deletion mutant, which lacks the N-terminal binding site for chaperone-subunit complexes (data not shown). Having verified our assay, we next measured binding of PapDG to the F21A and R652A PapC mutants. The apparent K_d of PapC F21A for PapDG was 62 nM (Fig. 4B), which is essentially identical to the K_d for WT PapC. However, the K_d of PapC R652A for PapDG was 1593 nM (Fig. 4C), which represents a 27-fold reduction in affinity. Note that in contrast to these results, the overlay assay reported weaker binding of PapDG to the F21A mutant compared to WT PapC (Fig. 3A). In the overlay assay, the usher

is bound to the PVDF membrane and this may limit protein-protein interactions. Indeed, our experience with the overlay assay suggests that it primarily measures binding to the N-terminal domain of PapC (Shu Kin So and Thanassi, 2006). In contrast, the fluorescence-based assay should allow for unhindered interactions. It is possible that the F21A mutation affects binding of PapDG to the N-terminal domain, but does not alter the overall affinity of PapDG for the usher due to interactions with additional regions of PapC, such as with the C-terminal domain.

We next tested binding of the PapC usher to PapDA chaperone-rod subunit complexes. PapA will spontaneously self-oligomerize through donor strand exchange interactions between the Nte of one PapA and the pilin domain of another PapA. To prevent this, we expressed and purified PapDA complexes using a $PapA_{NteK}$ variant, in which the PapA Nte was swapped with the Nte from PapK, which does not bind to PapA (Lee *et al.*, 2007; Rose *et al.*, 2008). Using our fluorescence-based assay, we measured an apparent K_d of 1527 nM for $PapDA_{NteK}$ binding to WT PapC (Fig. 5A). This matches the K_d value of 1.5 mM previously determined by surface plasmon resonance for $PapDA_{G150T}$ (the G150T mutation also prevents PapAoligomerization) (Saulino *et al.*, 1998). In comparison to the WT usher, affinity of the PapC F21A mutant for $PapDA_{NteK}$ was increased by approximately 2-fold (K_d = 648 nM) whereas affinity of PapC R652A was decreased by approximately 2-fold (K_d = 2520 nM) (Fig. 5B and C). Thus, both PapC mutations alter affinity of the usher for PapDA complexes, but in opposite directions.

The results of the PapDG and PapDA binding measurements support our proposed model that residues F21 and R652 are important for the ability of PapC to discriminate among chaperone-subunit complexes, and reveal distinct functions for the N- and C-terminal domains in the differential affinity of the usher. The R652A mutation in the usher C-terminal domain caused a 2-fold decrease in affinity for PapDA and a 27-fold decrease in affinity for PapDG. Therefore, the C-terminal domain is critical for the high affinity binding of chaperone-adhesin complexes to the usher. These data fit well with the previously identified ability of the isolated C-terminal domain to directly bind PapDG in an overlay assay, and with the model that the adhesin contacts the C-terminal domain following initial targeting to the N-terminal domain (Saulino *et al.*, 1998; Shu Kin So and Thanassi, 2006). The weaker binding of PapDA to PapC R652A is also in agreement with the proposed role of the C-terminal domain in stabilizing the binding of subunits to the usher (Shu Kin So and Thanassi, 2006). The inability of PapC R652A to assemble complete pili can be explained by the much greater decrease in affinity for PapDG compared to PapDA. When PapA is present, it will outcompete PapG for binding to the mutant usher. This will result in a complete absence of pili, because the PapA subunit cannot initiate pilus biogenesis (Jacob-Dubuisson *et al.*, 1993).

In contrast to PapC R652A, the F21A mutation in the usher N-terminal domain did not affect binding to PapDG, but caused increased affinity for PapDA complexes, suggesting that residue F21 is important for discrimination against PapA subunits. The increased affinity of the F21A mutant presumably allows PapDA complexes, when present at high concentration in the periplasm, to block PapDG and the other tip subunits from binding to the usher to initiate pilus assembly. Thus, PapC F21A can assemble pilus tips in the absence of PapA, but no pilus structures are assembled when PapA is present. In the co-crystal structure of the FimD N-terminal domain bound to a FimC chaperone-FimH pilin domain complex, residue F22 of FimD makes direct contact with the chaperone only (Nishiyama *et al.*, 2005). If PapC F21 similarly only contacts the chaperone, this would suggest that the effect of the F21A mutation on differential affinity of the usher is indirect, since the chaperone is the same for all pilus subunits. Alternatively, the lack of an effect of the F21A mutation on PapDG binding may indicate that the affinity of the usher for the adhesin is

primarily determined by additional interactions, such as with the usher C-terminal domain. These additional interactions may be specific for the adhesin, because the adhesin contains two domains (pilin domain and adhesin domain), whereas all other subunits contain only the single pilin domain.

The PapG adhesin is not required for assembly of P pili

In the type 1 pilus system, the FimH adhesin is required to initiate pilus biogenesis; no pili are assembled in the absence of the adhesin (Shu Kin So and Thanassi, 2006; Munera *et al.*, 2007; Nishiyama *et al.*, 2008). In contrast, previous studies suggested that PapG is not required to initiate P pilus biogenesis and that the PapF and PapK subunits may perform this function instead (Lindberg *et al.*, 1984; Kuehn *et al.*, 1992; Jacob-Dubuisson *et al.*, 1993). However, these studies used plasmid-based expression systems and did not examine clean deletions of *papG*. To determine if PapG is required for P pilus biogenesis, we constructed a clean deletion of *papG* in plasmid pPAP5, which encodes the complete *pap* gene cluster from *E. coli* strain J96 (Lindberg *et al.*, 1984), creating plasmid pPAPΔG. In addition, we constructed a clean deletion of *papG* in strain ZAP594, which contains the J96 *pap* gene cluster integrated into the chromosome (Holden *et al.*, 2007), creating strain ZAP594ΔpapG. We then examined the WT and Δ*papG* gene clusters for ability to assemble P pili. For this analysis, strains ZAP594 and ZAP594ΔpapG were transformed with plasmid pHGM98, encoding the *papI* regulator, to increase the off-to-on phase transition of the chromosomal *pap* gene cluster (Holden *et al.*, 2007). As expected, bacteria harboring the Δ*papG* gene clusters were unable to agglutinate human red blood cells (data not shown). However, both the plasmid- and chromosomal-based Δ*papG* gene clusters assembled similar amounts of pili as the WT *pap* gene clusters, as assessed by purification of pili from the bacterial surface (Fig. 6A). In addition, examination of whole bacteria by electron microscopy revealed similar numbers and appearance of pili between the WT and Δ*papG* strains (Fig. 6B). Thus, the PapG adhesin is not required to initiate P pilus biogenesis.

In the type 1 pilus system, the requirement for the adhesin to initiate pilus biogenesis ensures that only adhesive fibers are assembled on the bacterial surface. The fact that P pili lack this mechanism is surprising, as the adhesin is essential for pilus function in host cell colonization (Roberts *et al.*, 1994). Our results suggest that the preferential affinity of the usher for the adhesin is critical in P pilus biogenesis to ensure the assembly of functional pilus fibers. In the type 1 pilus system, binding of chaperone-adhesin complexes to the usher causes a conformational change that may activate the usher for pilus biogenesis (Saulino *et al.*, 1998). This conformational change may involve gating open of the usher channel and activation of the usher's catalytic activity (Nishiyama *et al.*, 2008; Remaut *et al.*, 2008). PapC may already be in an activated state and thus not require priming by the adhesin. Alternatively, the PapF and PapK tip subunits may serve as activators of the usher, as suggested by previous studies (Jacob-Dubuisson *et al.*, 1993). Given that PapG is not required for P pilus assembly, the inability of the PapC F21A and R652A mutants to assemble pili in the presence of PapA suggests that the other tip subunits are also blocked from binding to the mutant ushers. This would be expected, since the other tip subunits have weaker binding affinities for the usher compared to the PapG adhesin (Dodson *et al.*, 1993).

Conclusions

We show here that PapC F21A and R652A mutants are defective for pilus biogenesis when the PapA rod subunit is present, even though these mutants are functional for assembly of pilus tips in the absence of PapA. Using an in vitro, fluorescence-based assay, we show that the PapC F21A and R652A mutations affect the differential affinity of the usher for chaperone-subunit complexes. Although we do know yet if resides F21 and R652 make direct contacts with chaperone-subunit complexes, our results suggest distinct functions for

the usher N-and C-terminal domains in discrimination among pilus subunits, with residue F21 in the N-terminal domain important for restricting affinity for PapA rod subunits and residue R652 in the C-terminal domain important for promoting high affinity binding to the PapG adhesin. Our findings suggest that the differential affinity of the usher for chaperone-subunit complexes is required to allow assembly of complete pili. Thus, the differential affinity of the usher may have evolved to balance the necessity to have high concentrations of PapA subunits available in the periplasm to build the pilus rods with the need to have the minor tip components assembled first. Precise measurements of the concentrations of the different chaperone-subunit complexes in the periplasm along with determinations of the binding affinities for all chaperone-subunit complexes will be required to generate a detailed model for ordered pilus biogenesis at the OM usher. Pilus biogenesis is a complex, multi-stage process and factors in addition to affinity for the usher must be taken into consideration. For example, the binding of a chaperone-subunit complex to the usher may influence affinity for the next chaperone-subunit complex. In addition, the capacity of only some subunits (PapG, F and K) to serve as initiators of pilus biogenesis places important restrictions on the overall assembly process. This fact is emphasized by the absence of pilus rods on the bacterial surface in the PapC F21A and R652A mutants; PapDA complexes may bind to the ushers, but PapA cannot initiate pilus assembly. Recent studies demonstrated that subunit ordering in the pilus fiber is in part governed by the donor strand exchange reaction (Lee *et al.*, 2007; Rose *et al.*, 2008). The differential affinity of the usher, combined with the initiator function of only certain subunits, likely determines which subunit initiates pilus assembly. Once the initial subunit is bound to the usher, the donor strand exchange reaction may then drive the subsequent ordering of subunits during pilus elongation. In the type 1 pilus system, only the adhesin can initiate pilus biogenesis, ensuring that only adhesive fibers are assembled. Since PapG is not required to initiate P pilus biogenesis, this suggests that the differential affinity of the usher is particularly critical in the P pilus system to ensure the assembly of functional pili.

EXPERIMENTAL PROCEDURES

Strains and plasmids

The bacterial strains and plasmids used in this study are listed in Table 3. Unless otherwise indicated, all strains were grown at 37°C with aeration in Luria-Bertani (LB) medium with appropriate antibiotics. DH5α was used as the host strain for plasmid manipulations and all mutants were sequenced to verify the intended mutation.

Plasmid pMJ3 contains the *papC* usher gene with a hexahistidine tag (His-tag) appended to its C terminus, under control of the arabinose (P_{ara}) promoter (Thanassi *et al.*, 1998). Plasmids pTN51 and pTN52, containing PapC substitution mutations F18A and F21A, respectively, were derived from plasmid pMJ3 using the QuikChange Site-Directed Mutagenesis Kit (Stratagene) and the primers listed in Table S1. Plasmids pTN35, pQY21 and pQY652 were derived from pAP3 (PapC Δ2-11), pTN52 (PapC F21A) and pSS21 (PapC R652A) (Shu Kin So and Thanassi, 2006), respectively, using the QuikChange Site-Directed Mutagenesis Kit and primers listed in Table S1 to insert a thrombin cleavage site (LVPRGS) between the PapC C-terminus and the His-tag. Plasmid pNH200, encoding *papD* under control of P_{ara} in vector pMON6235Δcat was derived from pHJ9210 (Jones *et al.*, 1997) using the QuikChange Site-Directed Mutagenesis Kit and the primers listed in Table S1 to insert a thrombin cleavage site between the PapD C-terminus and a C-terminal His-tag.

Plasmid pPAPDA, encoding the *papD* and *papA* genes under control of P_{ara} was constructed as follows. *PapA* was cut from plasmid pHJ2 (Jacob-Dubuisson *et al.*, 1994a) using SmaI and SalI, and then ligated into vector pBAD18-cm that had been similarly

digested, creating plasmid pTN45. *PapD* was cut from plasmid pLS101 (Slonim *et al.*, 1992) using EcoRI and SalI, and then ligated into vector pBAD18-kan that had been similarly digested, creating plasmid pTN11. Plasmid pTN11 was then digested with NheI and SalI, the *papD* fragment blunt ended with T4 DNA polymerase, and the fragment ligated into pTN45 that had been digested with KpnI and blunt ended, creating pPAPDA.

Plasmid pDGT10, encoding *papC* in vector pACYC184 under control of the IPTG-inducible promoter P_{trc}, was constructed as follows. *PapC* was cut from plasmid pFJ20 (Jacob-Dubuisson *et al.*, 1994b) with SmaI and BglII, blunt ended with T4 polymerase, and then ligated into plasmid pFJ29 (Jacob-Dubuisson *et al.*, 1994b) that had been digested with AvaI, ScaI and NsiI and blunt ended. Plasmids pSSF21A and pSSR652A were derived from plasmid pDGT10 using the QuikChange Site-Directed Mutagenesis Kit and the primers listed in Table S1 to introduce the PapC F21A and R652A mutations, respectively.

Plasmid pTN17, encoding class II *papG* under control of the IPTG-inducible promoter P_{tac}, was constructed as follows. *PapGII* was cut from plasmid pTrcGII (Dodson *et al.*, 2001) with EcoRI and BamHI, and then ligated into plasmid pMMB66 that had been similarly digested.

Plasmid pTRYC-K1A was made by standard two-step PCR and the primers listed in Table S1 to create a gene product encoding the Nte of PapK fused to the pilin domain of PapA. This gene product was cloned into the polylinker region (via EcoRI and BamHI digestion) of a chimeric vector called pTRYC, which contains the chloramphenicol resistance gene and plasmid origin regions from vector pACYC184 and the lacIq and polylinker regions from vector pTRC99A.

Plasmid pPAPΔG was derived from plasmid pPAP5 (Lindberg *et al.*, 1984), which contains the complete *pap* gene cluster from strain J96 under control of its native promoter in vector pBR322, as follows. ABamHI restriction site was introduced in the intergenic region between *papF* and *papG* in pPAP5 using the QuikChange Site-Directed Mutagenesis Kit and the primers listed in Table S1. The complete *papG* gene was then deleted by digesting the resulting plasmid with BamHI and religating, creating plasmid pPAPΔG.

The *papG* deletion in strain ZAP594 was constructed using the λ Red recombinase method (Datsenko and Wanner, 2000) and the primers listed in Table S1. Strain ZAP594 contains the J96 *pap* gene cluster integrated into the chromosome of the *E. coli* K12 strain MG1655 (Holden *et al.*, 2007). The *papG* gene of ZAP594 was first replaced with a kanamycin-resistant cassette, and the cassette was then eliminated using FLP recombinase, generating strain ZAP594ΔpapG. Proper construction of the intermediate and final strains was confirmed by PCR.

OM isolation and analysis of PapC expression and folding

Strain SF100 harboring the appropriate PapC expression plasmid was induced at OD_{600} = 0.6 with 0.1% L-arabinose for 1 h. OM fractions were isolated by French press disruption and Sarkosyl extraction, as described (Ng *et al.*, 2004; Shu Kin So and Thanassi, 2006). Expression levels of the PapC proteins in the OM were determined by immunoblotting with anti-His-tag (Covance) or anti-PapC antibodies. Immunoblots were developed with the appropriate alkaline phosphatase-conjugated secondary antibody and BCIP (5-bromo-4-chloro-3-indolylphosphate)-NBT (nitroblue tetrazolium) substrate (KPL). Proper folding of the PapC proteins in the OM was checked by resistance to denaturation by SDS, which provides an indication of proper folding and stability of the β-barrel domain (Sugawara *et al.*, 1996). This was determined by heat-modifiable mobility on SDS-PAGE, performed as described (Ng *et al.*, 2004; Shu Kin So and Thanassi, 2006).

Hemagglutination assay

Hemagglutination assays were performed as described (Shu Kin So and Thanassi, 2006). For analysis of assembly of complete pili, AAEC185/pMJ2 (Δ*papC pap* operon; *papAHDJKEFG*) was used as the host strain. For analysis of assembly of pilus tips, AAEC185/pPAP58 (*papDJKEFG*) was used as the host strain. The host strains harboring the appropriate PapC expression plasmids were induced at OD_{600} = 0.6 with 0.1% L-arabinose and mM isopropyl-β-D-thiogalactoside (IPTG) for 1 h. The hemagglutination titer was determined serial dilution in microtiter plates, with the titer calculated as the highest fold dilution of bacteria still able to agglutinate human red blood cells. The assay was performed in triplicate.

Hemagglutination assays to determine the effect of PapDA expression on pilus assembly were performed as above, with the following modifications. Host strain AAEC185/pPAP58 (*papDJKEFG)* + pPAPDA (*papDA*) harboring the appropriate PapC expression plasmid was induced with 0.1 mM IPTG (for expression of PapC and the pilus tip subunits) and either 0, 0.05, 0.1 or 0.5% L-arabinose (for expression of PapDA).

Purification of pili from the bacterial surface

P pili were isolated from host strain AAEC185/pMJ2 (Δ*papC pap* operon) harboring the appropriate PapC expression plasmid by heat extraction and magnesium precipitation, as described (Shu Kin So and Thanassi, 2006). Bacteria were induced at OD_{600} = 0.6 with 0.1% L-arabinose and 0.1 mM isopropyl-β-D-thiogalactoside (IPTG) for 1 h. Purified pili were examined by SDS-PAGE, followed by Coomassie blue staining to detect the major pilin PapA, or immunoblotting with anti-P pilus tips antiserum to detect the tip subunits PapG, F and E. For assays to determine the effect of PapDA expression on pilus assembly, strains were grown as described above for the hemagglutination assay.

Purification of pili from the *papG* chromosomal deletion strains (AAEC185/pPAP5, AAEC185/pPAPΔG, ZAP594/pHBM98 and ZAP594ΔpapG/pHGM98) was performed as above, except the bacteria were grown on CFA (colonization factor antigen) agar (Evans *et al.*, 1977) for 3 passages at 37°C.

Electron microscopy

Whole-bacteria, negative-stain transmission electron microscopy was performed as described (Ng *et al.*, 2004). Strains AAEC185/pPAP5, AAEC185/pPAPΔG, ZAP594/pHBM98 and ZAP594ΔpapG/pHGM98 were grown on CFAagar as described above. The electron microscopy grids were examined on an FEI TECNAI 12 BioTwin G02 microscope (FEI) at 80 kV accelerating voltage. Digital images were acquired with an AMT XR-60 CCD digital camera system (Advanced Microscopy Techniques).

Overlay assay

Overlay assays were performed as described (Shu Kin So and Thanassi, 2006). OM fractions were isolated from strain SF100 harboring the appropriate PapC expression plasmid as described above. The OM fractions were subjected to SDS-PAGE, transferred to a PVDF (polyvinylidene difluoride; Osmonics) membrane, and incubated with periplasm fractions containing PapDG. The periplasm fractions were isolated from strain SF100/pJP1 (PapDG) as described (Ng *et al.*, 2004). Binding of PapDG to PapC on the PVDF membrane was detected by immunobloting with anti-PapDG antibody.

Co-purification of pilus subunits with PapC

Co-purification assays were performed as described (Shu Kin So and Thanassi, 2006). OM fractions were isolated from strain SF100/pPAP58 (*papDJKEFG*) harboring the appropriate PapC expression plasmid as described above. The OM fractions were solubilized with the nondenaturing detergent dodecyl-maltopyranoside (DDM; Anatrace) and subjected to nickel affinity chromatography. PapC was eluted from the nickel column using an imidazole step gradient. Fractions containing PapC were subjected to SDS-PAGE and either stained with Coomassie blue to detect PapC or immunoblotted with anti-P pilus tips antiserum to detect pilus tip subunits that co-purified with the usher.

Protein Purification

The PapC ushers were purified as follows. OM fractions were isolated as described above from strain SF100 harboring WT PapC (pDG2), PapC Δ2-11 (pTN35), PapC F21A (pQY21) or PapC R652A (pQY652). The OM was solubilized by resuspending in 20 mM Tris-HCl (pH 8), 0.12 M NaCl and 1% DDM, and rocking overnight at 4oC. Insoluble material was removed by centrifugation (80,000 *g*, 45 min, 4oC), imadazole was added to 20 mM to the supernatant fraction and this fraction was run over a nickel affinity column (HisTrap; GE Healthcare) using an Akta FPLC apparatus (GE Healthcare). The bound PapC protein was eluted using an imidazole step gradient in buffer A [20 mM Tris-HCl (pH 8), 0.12 M NaCl and 10 mM lauryl(dimethyl)amine oxide (LDAO; Anatrace)]. Fractions containing PapC were pooled and the His-tag was cleaved off PapC by overnight digestion at room temperature with 10 units thrombin per mg PapC while dialyzing against 20 mM Tris-HCl (pH 8) and 0.12 M NaCl. The thrombin was inhibited by addition of PMSF and the mixture was subjected to a second round of chromatography in buffer A using a HisTrap column directly linked to a HiTrap benzamidine column (GE Healthcare). In this case, the thrombin-cleaved PapC came off the columns in the flow-through fraction, whereas uncleaved PapC, contaminants and the thrombin remained bound to the columns. The collected flow-through material was dialyzed into 20 mM Hepes (pH 7.5), 150 mM NaCl and 5 mM LDAO, and concentrated using a Millipore Ultrafree centrifugal concentrator (50 kDa molecular weight cutoff). Protein concentrations were determined using the bicinchoninic acid (BCA) protein assay (Pierce).

PapD and PapDG were purified as follows. Strains Tuner/pNH200 (His-tagged PapD) and Tuner/pNH200 + pTN17 (PapG) were induced with 0.01% L-arabinose for PapD expression and 1 mM IPTG for PapG expression, and periplasm fractions were isolated as described (Ng *et al.*, 2004). The periplasms were dialyzed into 20 mM Tris (pH 8) and 0.3 M NaCl, imidazole was added to 20 mM, and the samples were run over a nickel affinity column (HisTrap) using an Akta FPLC apparatus. The bound proteins were eluted using an imidazole step gradient, and fractions containing the purified PapD or PapDG were dialyzed into 20 mM MES (pH 5.8). The samples were then subjected to an additional chromatography step using a Resource S ion exchange column (GE Healthcare) and eluted using a NaCl gradient.

For purification of PapDA, strain C600/pDF1 (His-tagged PapD) + pTRYC-K1A ($PapA_{NteK}$; PapA pilin domain with PapK Nte) was grown in a 5 L fermentor in Brain Heart Infusion (BHI)/LB and induced with 0.2 mM IPTG. The periplasm fraction was isolated, dialyzed against 1X phosphate buffered saline plus 250 mM NaCl, and then run on a Talon metal affinity column (Clontech). The bound proteins were eluted with an imidazole gradient, and the fractions containing $PapDA_{NteK}$ were pooled and dialyzed against 15 mM MES (pH 6.0), and then run on an S column and eluted with a NaCl gradient. The fractions containing $PapDA_{NteK}$ were pooled, ammonium sulfate was added to 0.8 M, and the sample was subjected to a final chromatography step using a Phenyl hydrophobic interaction

column (GE Healthcare). The protein was eluted using a decreasing ammonium sulfate gradient, and the fractions containing the final purified $PapDA_{NteK}$ complex were pooled and dialyzed into 15 mM MES (pH 6.0).

In vitro fluorescence-based assay for quantification chaperone-subunit binding to the usher

Measurements of binding affinities to the usher were conducted essentially as described (Royer and Scarlata, 2008). Purified chaperone or chaperone-subunit complexes were labeled with the amine-reactive probe coumarin SE (DMACA, SE; Invitrogen). For labeling, the pH of the protein solution was first raised to 8.0 by addition of K_2HPO_4, and then probe was added at a 5:1 probe:protein molar ratio and the mixture incubated for 45 min at 4oC. The solution was dialyzed at 4°C against at least 3 changes of 20 mM Hepes (pH 7.5), 150 mM NaCl to remove unreacted probe, followed by a final overnight dialysis against 20 mM Hepes (pH 7.5), 150 mM NaCl and 5 mM LDAO to put the labeled proteins into the same buffer as the purified PapC. The labeling efficiency was checked by comparing protein absorbance at 280 nm with absorbance of the probe at 376 nm. Under these conditions, a labeling ratio of 0.8–1.0 mol probe/mol protein was obtained.

Fluorescence measurements were performed at room temperature using a PC1 photon counting spectrofluorometer (ISS). The coumarin-labeled chaperone or chaperone-subunit complex was diluted to 25 nM final concentration using 20 mM Hepes (pH 7.5), 150 mM NaCl and 5 mM LDAO, and 120 μl was transferred to a 3 mm microcuvette. Purified PapC was then titrated into the cuvette and spectra were recorded using a 376 nm excitation wavelength and by scanning emission values from 420 to 520 nm. The area under the curve was calculated to give the total emission intensity. Corrections for background scatter were made by subtracting out intensity values obtained by titrating with buffer only, and corrections for dilution were made to account for changes in volume during PapC titration. The values were normalized to present the data as the fraction of protein bound as a function of added PapC, with the starting value (no PapC added) set to 0 and the final value (highest concentration of PapC added) set to 1. Apparent equilibrium bimolecular dissociation constants (K_d) were then obtained by fitting the data to a titration curve using the sigmoidal curve-fitting function in SigmaPlot (Systat Software). Each titration curve represents the average of at least three independent experiments, with one-to-three replicates per experiment.

Acknowledgments

We thank David L. Gally (University of Edinburgh, UK) for providing strain ZAP594 and plasmid pHGM98. We thank Susan Van Horn and the Central Microscopy Imaging Center (Stony Brook University) for assistance with electron microscopy. We thank Wali Karzi (Stony Brook University) for helpful discussions. This work was supported by NIH grants GM062987 (to D.G.T.), GM053132 (to S.S.), and AI029549 and AI048689 (to S.J.H.)

References

Baga M, Goransson M, Normark S, Uhlin BE. Processed mRNA with differential stability in the regulation of E. coli pilin gene expression. Cell. 1988; 52:197–206. [PubMed: 2449283]

Baga M, Norgren M, Normark S. Biogenesis of *E. coli* Pap pili: PapH, a minor pilin subunit involved in cell anchoring and length modulation. Cell. 1987; 49:241–251. [PubMed: 2882856]

Baneyx F, Georgiou G. In vivo degradation of secreted fusion proteins by the Escherichia coli outer membrane protease OmpT. J Bacteriol. 1990; 172:491–494. [PubMed: 2403549]

Blomfield IC, McClain MS, Eisenstein BI. Type 1 fimbriae mutants of Escherichia coli K12: characterization of recognized afimbriate strains and construction of new fim deletion mutants. Mol Microbiol. 1991; 5:1439–1445. [PubMed: 1686292]

Campbell A. Sensitive mutants of bacteriophage lambda. Virology. 1961; 14:22–32. [PubMed: 13690195]

Choudhury D, Thompson A, Stojanoff V, Langermann S, Pinkner J, Hultgren SJ, Knight SD. X-ray structure of the FimC-FimH chaperone-adhesin complex from uropathogenic *Escherichia coli*. Science. 1999; 285:1061–1066. [PubMed: 10446051]

Datsenko KA, Wanner BL. One-step inactivation of chromosomal genes in Escherichia coli K-12 using PCR products. Proc Natl Acad Sci U S A. 2000; 97:6640–6645. [PubMed: 10829079]

Dodson KW, Jacob-Dubuisson F, Striker RT, Hultgren SJ. Outer membrane PapC usher discriminately recognizes periplasmic chaperone-pilus subunit complexes. Proc Natl Acad Sci U S A. 1993; 90:3670–3674. [PubMed: 8097321]

Dodson KW, Pinkner JS, Rose T, Magnusson G, Hultgren SJ, Waksman GJ. Structural basis of the Interaction of the pyelonephritic *E. coli* adhesin to Its human kidney receptor. Cell. 2001; 105:733–743. [PubMed: 11440716]

Driessen AJ, Nouwen N. Protein translocation across the bacterial cytoplasmic membrane. Annu Rev Biochem. 2008; 77:643–667. [PubMed: 18078384]

Evans DG, Evans DJ Jr, Tjoa W. Hemagglutination of human group A erythrocytes by enterotoxigenic *Escherichia coli* isolated from adults with diarrhea: correlation with colonization factor. Infect Immun. 1977; 18:330–337. [PubMed: 336541]

Foxman B, Brown P. Epidemiology of urinary tract infections: transmission and risk factors, incidence, and costs. Infect Dis Clin North Am. 2003; 17:227–241. [PubMed: 12848468]

Grant SG, Jessee J, Bloom FR, Hanahan D. Differential plasmid rescue from transgenic mouse DNAs into Escherichia coli methylation-restriction mutants. Proc Natl Acad Sci U S A. 1990; 87:4645–4649. [PubMed: 2162051]

Holden N, Totsika M, Dixon L, Catherwood K, Gally DL. Regulation of P-fimbrial phase variation frequencies in *Escherichia coli* CFT073. Infect Immun. 2007; 75:3325–3334. [PubMed: 17452474]

Hultgren SJ, Lindberg F, Magnusson G, Kihlberg J, Tennent JM, Normark S. The PapG adhesin of uropathogenic Escherichia coli contains separate regions for receptor binding and for the incorporation into the pilus. Proc Natl Acad Sci U S A. 1989; 86:4357–4361. [PubMed: 2567514]

Jacob-Dubuisson F, Heuser J, Dodson K, Normark S, Hultgren SJ. Initiation of assembly and association of the structural elements of a bacterial pilus depend on two specialized tip proteins. EMBO J. 1993; 12:837–847. [PubMed: 8096174]

Jacob-Dubuisson F, Pinkner J, Xu Z, Striker R, Padmanhaban A, Hultgren SJ. PapD chaperone function in pilus biogenesis depends on oxidant and chaperone-like activities of DsbA. Proc Natl Acad Sci USA. 1994a; 91:11552–11556. [PubMed: 7972100]

Jacob-Dubuisson F, Striker R, Hultgren SJ. Chaperone-assisted self-assembly of pili independent of cellular energy. J Biol Chem. 1994b; 269:12447–12455. [PubMed: 7909802]

Jones CH, Danese PN, Pinkner JS, Silhavy TJ, Hultgren SJ. The chaperone-assisted membrane release and folding pathway is sensed by two signal transduction systems. EMBO J. 1997; 16:6394–6406. [PubMed: 9351822]

Kuehn MJ, Heuser J, Normark S, Hultgren SJ. P pili in uropathogenic *E. coli* are composite fibres with distinct fibrillar adhesive tips. Nature. 1992; 356:252–255. [PubMed: 1348107]

Lee YM, Dodson KW, Hultgren SJ. Adaptor function of PapF depends on donor strand exchange in P-pilus biogenesis of Escherichia coli. J Bacteriol. 2007; 189:5276–5283. [PubMed: 17496084]

Li H, Qian L, Chen Z, Thahbot D, Liu G, Liu T, Thanassi DG. The outer membrane usher forms a twin-pore secretion complex. J Mol Biol. 2004; 344:1397–1407. [PubMed: 15561151]

Li H, Thanassi DG. Use of a combined cryo-EM and X-ray crystallography approach to reveal molecular details of bacterial pilus assembly by the chaperone/usher pathway. Curr Opin Microbiol. 2009; 12:326–332. [PubMed: 19356973]

Lindberg FP, Lund B, Normark S. Genes of pyelonephritogenic E. coli required for digalactoside-specific agglutination of human cells. EMBO J. 1984; 3:1167–1173. [PubMed: 6145590]

Lund B, Lindberg F, Marklund BI, Normark S. The PapG protein is the α-D-galactopyranosyl-(1-4)-β-D-galactopyranose-binding adhesin of uropathogenic *Escherichia coli*. Proc Natl Acad Sci USA. 1987; 84:5898–5902. [PubMed: 2886993]

Mapingire OS, Henderson NS, Duret G, Thanassi DG, Delcour AH. Modulating effects of the plug, helix and N- and C-terminal domains on channel properties of the PapC usher. J Biol Chem. 2009 in press.

Mu XQ, Bullitt E. Structure and assembly of P-pili: a protruding hinge region used for assembly of a bacterial adhesion filament. Proc Natl Acad Sci U S A. 2006; 103:9861–9866. [PubMed: 16782819]

Munera D, Hultgren S, Fernandez LA. Recognition of the N-terminal lectin domain of FimH adhesin by the usher FimD is required for type 1 pilus biogenesis. Mol Microbiol. 2007; 64:333–346. [PubMed: 17378923]

Ng TW, Akman L, Osisami M, Thanassi DG. The usher N terminus is the initial targeting site for chaperone-subunit complexes and participates in subsequent pilus biogenesis events. J Bacteriol. 2004; 186:5321–5331. [PubMed: 15292133]

Ng TW, Akman L, Osisami M, Thanassi DG. Author's Correction: The usher N terminus is the initial targeting site for chaperone-subunit complexes and participates in subsequent pilus biogenesis events. J Bacteriol. 2006; 188:2295.

Nishiyama M, Horst R, Eidam O, Herrmann T, Ignatov O, Vetsch M, Bettendorff P, Jelesarov I, Grutter MG, Wuthrich K, Glockshuber R, Capitani G. Structural basis of chaperone-subunit complex recognition by the type 1 pilus assembly platform FimD. EMBO J. 2005; 24:2075–2086. [PubMed: 15920478]

Nishiyama M, Ishikawa T, Rechsteiner H, Glockshuber R. Reconstitution of Pilus Assembly Reveals a Bacterial Outer Membrane Catalyst. Science. 2008; 320:376–379. [PubMed: 18369105]

Nishiyama M, Vetsch M, Puorger C, Jelesarov I, Glockshuber R. Identification and characterization of the chaperone-subunit complex-binding domain from the type 1 pilus assembly platform FimD. J Mol Biol. 2003; 330:513–525. [PubMed: 12842468]

Norgren M, Baga M, Tennent JM, Normark S. Nucleotide sequence, regulation and functional analysis of the papC gene required for cell surface localization of Pap pili of uropathogenic Escherichia coli. Mol Microbiol. 1987; 1:169–178. [PubMed: 2897064]

Remaut H, Tang C, Henderson NS, Pinkner JS, Wang T, Hultgren SJ, Thanassi DG, Waksman G, Li H. Fiber Formation across the Bacterial Outer Membrane by the Chaperone/Usher Pathway. Cell. 2008; 133:640–652. [PubMed: 18485872]

Roberts JA, Marklund BI, Ilver D, Haslam D, Kaack MB, Baskin G, Louis M, Mollby R, Winberg J, Normark S. The Galα(1-4)Gal-specific tip adhesin of *Escherichia coli* P-fimbriae is needed for pyelonephritis to occur in the normal urinary tract. Proc Natl Acad Sci USA. 1994; 91:11889–11893. [PubMed: 7991552]

Rose RE. The nucleotide sequence of pACYC184. Nucleic Acids Res. 1988; 16:355. [PubMed: 3340533]

Rose RJ, Verger D, Daviter T, Remaut H, Paci E, Waksman G, Ashcroft AE, Radford SE. Unraveling the molecular basis of subunit specificity in P pilus assembly by mass spectrometry. Proc Natl Acad Sci U S A. 2008; 105:12873–12878. [PubMed: 18728178]

Royer CA, Scarlata SF. Fluorescence approaches to quantifying biomolecular interactions. Methods Enzymol. 2008; 450:79–106. [PubMed: 19152857]

Sauer FG, Fütterer K, Pinkner JS, Dodson KW, Hultgren SJ, Waksman G. Structural basis of chaperone function and pilus biogenesis. Science. 1999; 285:1058–1061. [PubMed: 10446050]

Sauer FG, Pinkner JS, Waksman G, Hultgren SJ. Chaperone priming of pilus subunits facilitates a topological transition that drives fiber formation. Cell. 2002; 111:543–551. [PubMed: 12437927]

Sauer FG, Remaut H, Hultgren SJ, Waksman G. Fiber assembly by the chaperone-usher pathway. Biochim Biophys Acta. 2004; 1694:259–267. [PubMed: 15546670]

Saulino ET, Thanassi DG, Pinkner JS, Hultgren SJ. Ramifications of kinetic partitioning on usher-mediated pilus biogenesis. EMBO J. 1998; 17:2177–2185. [PubMed: 9545231]

Shu Kin So S, Thanassi DG. Analysis of the requirements for pilus biogenesis at the outer membrane usher and the function of the usher C-terminus. Mol Microbiol. 2006; 60:364–375. [PubMed: 16573686]

Slonim LN, Pinkner JS, Branden CI, Hultgren SJ. Interactive surface in the PapD chaperone cleft is conserved in pilus chaperone superfamily and essential in subunit recognition and assembly. EMBO J. 1992; 11:4747–4756. [PubMed: 1361168]

Sugawara E, Steiert M, Rouhani S, Nikaido H. Secondary structure of the outer membrane proteins OmpA of *Escherichia coli* and OprF of *Pseudomonas aeruginosa*. J Bacteriol. 1996; 178:6067–6069. [PubMed: 8830709]

Thanassi DG, Saulino ET, Lombardo MJ, Roth R, Heuser J, Hultgren SJ. The PapC usher forms an oligomeric channel: implications for pilus biogenesis across the outer membrane. Proc Natl Acad Sci U S A. 1998; 95:3146–3151. [PubMed: 9501230]

Thanassi DG, Stathopoulos C, Dodson KW, Geiger D, Hultgren SJ. Bacterial outer membrane ushers contain distinct targeting and assembly domains for pilus biogenesis. J Bacteriol. 2002; 184:6260–6269. [PubMed: 12399496]

Verger D, Miller E, Remaut H, Waksman G, Hultgren S. Molecular mechanism of P pilus termination in uropathogenic Escherichia coli. EMBO Rep. 2006; 7:1228–1232. [PubMed: 17082819]

Watson N. A new revision of the sequence of plasmid pBR322. Gene. 1988; 70:399–403. [PubMed: 3063608]

Wright KJ, Seed PC, Hultgren SJ. Development of intracellular bacterial communities of uropathogenic *Escherichia coli* depends on type 1 pili. Cell Microbiol. 2007; 9:2230–2241. [PubMed: 17490405]

Zavialov AV, Berglund J, Pudney AF, Fooks LJ, Ibrahim TM, MacIntyre S, Knight SD. Structure and biogenesis of the capsular F1 antigen from Yersinia pestis: preserved folding energy drives fiber formation. Cell. 2003; 113:587–596. [PubMed: 12787500]

Zavialov AV V, Tischenko M, Fooks LJ, Brandsdal BO, Aqvist J, Zav'yalov VP, Macintyre S, Knight SD. Resolving the energy paradox of chaperone/usher-mediated fibre assembly. Biochem J. 2005; 389:685–694. [PubMed: 15799718]

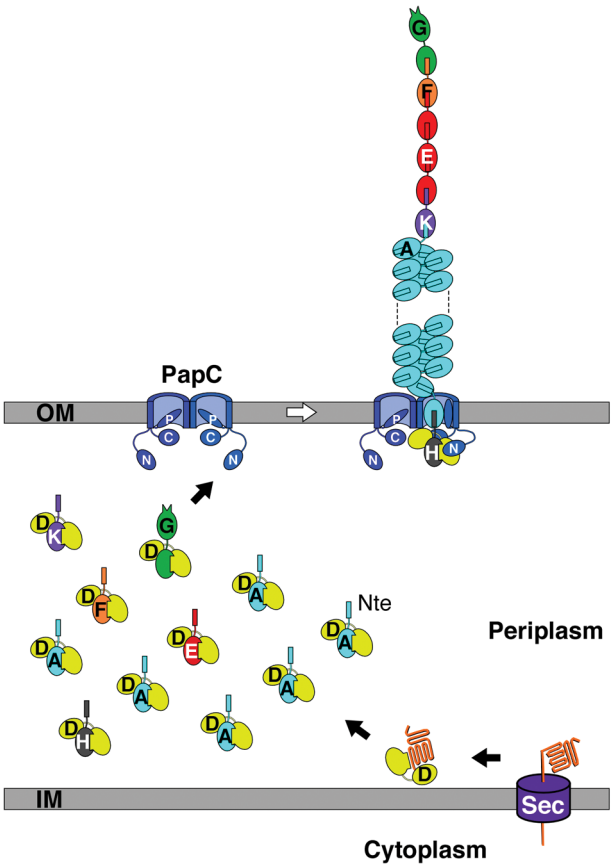

Fig. 1.

Model for the assembly and secretion of P pili by the CU pathway. The Pap proteins are represented by single letters (A, PapA; H, PapH; etc.). The dimeric PapC usher is depicted with the central β-barrel domain forming a channel that spans the OM, the N- and C-terminal domains (labeled N and C, respectively) located in the periplasm, and the plug domain (labeled P) gating the channel shut. Pilus subunits cross the inner membrane via the Sec general secretory pathway and then form binary complexes with the PapD chaperone. PapDG complexes have highest affinity for the usher and initiate pilus assembly by binding to the N-terminal domain of an usher monomer. The usher catalyzes subunit incorporation into the pilus fiber and allows secretion of the fiber to the cell surface.

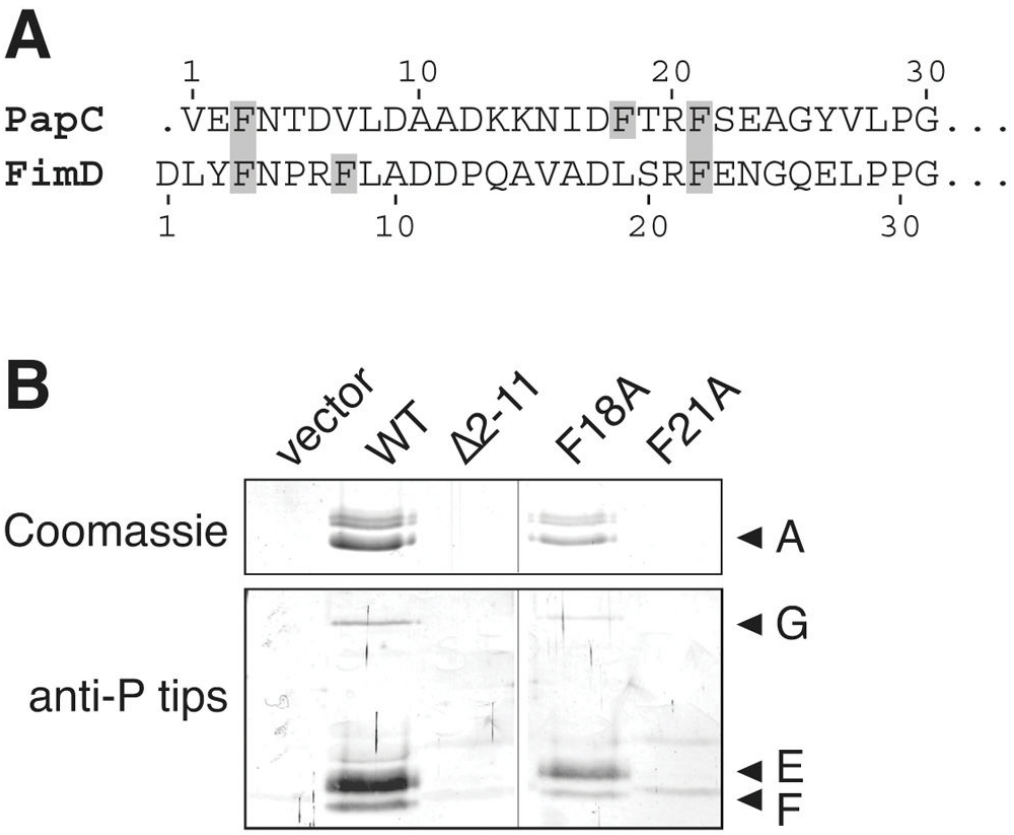

Fig. 2.

PapC F21 is required for P pilus assembly.

A. Alignment of the chaperone-subunit binding regions of the N-terminal domains of the PapC and FimD ushers. Phenylalanine residues are indicated with grey shading. Residue numbers relative to the mature N-termini of PapC and FimD are indicated above and below the alignment, respectively.

B. Pilus purification. Strain AAEC185/pMJ2 (Δ*papC pap* operon) was complemented with vector only, WT PapC, or the indicated PapC mutant. Pili were isolated from the bacterial surface by heat extraction and magnesium precipitation, and then subjected to SDS-PAGE. The PapA major rod subunit (A, upper panel) was visualized by Coomassie blue staining. Pilus tip subunits (PapG, E and F, lower panel) were detected by immunoblotting with anti-P pilus tips antiserum.

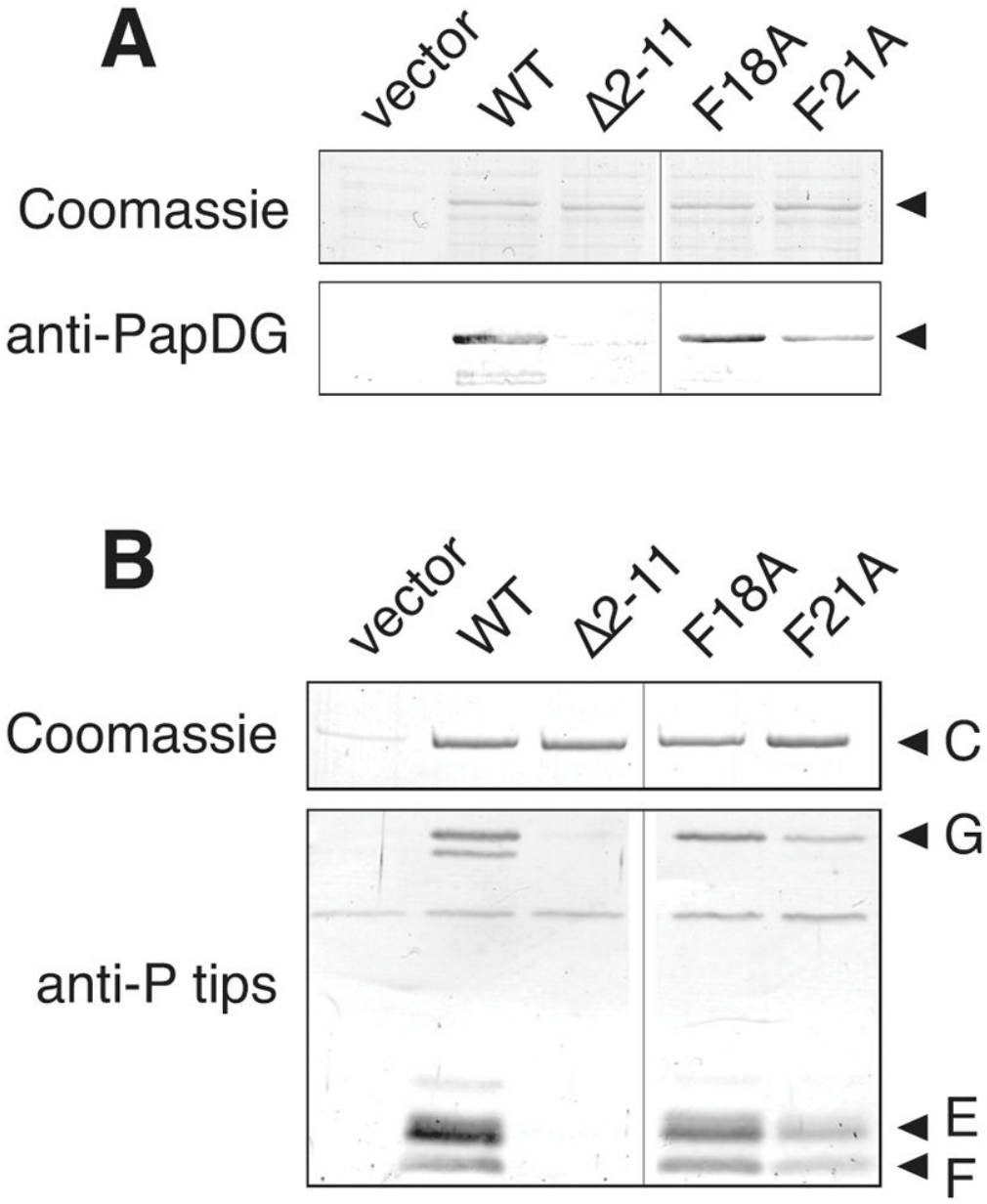

Fig. 3.

PapC F21A binds to pilus subunits in vitro and in vivo.

A. Overlay assay for binding of PapDG to PapC. OM fractions were isolated from strain SF100 expressing vector only, WT PapC, or the indicated PapC mutant. Duplicate samples were subjected to SDS-PAGE and either stained with Coomassie blue to show the amount of PapC present (arrow head, upper panel), or transferred to a PVDF membrane for the overlay assay. Binding of PapDG to the usher (arrow head, lower panel) was determined by immunoblotting with anti-PapDG antibody.

B. Co-purification of pilus tip subunits with the usher. OM fractions were isolated from strain SF100/pPAP58 (*papDJKEFG*) expressing vector only, WT PapC, or the indicated PapC mutant. OM fractions were solubilized with non-denaturing detergent and PapC was purified by affinity chromatography. The peak fraction containing PapC was subjected to SDS-PAGE and either stained with Coomassie blue to show the amount of PapC present (C,

upper panel) or immunoblotted with anti-P pilus tips antiserum to detect pilus tip subunits that co-purified with the usher (PapG, E and F, lower panel).

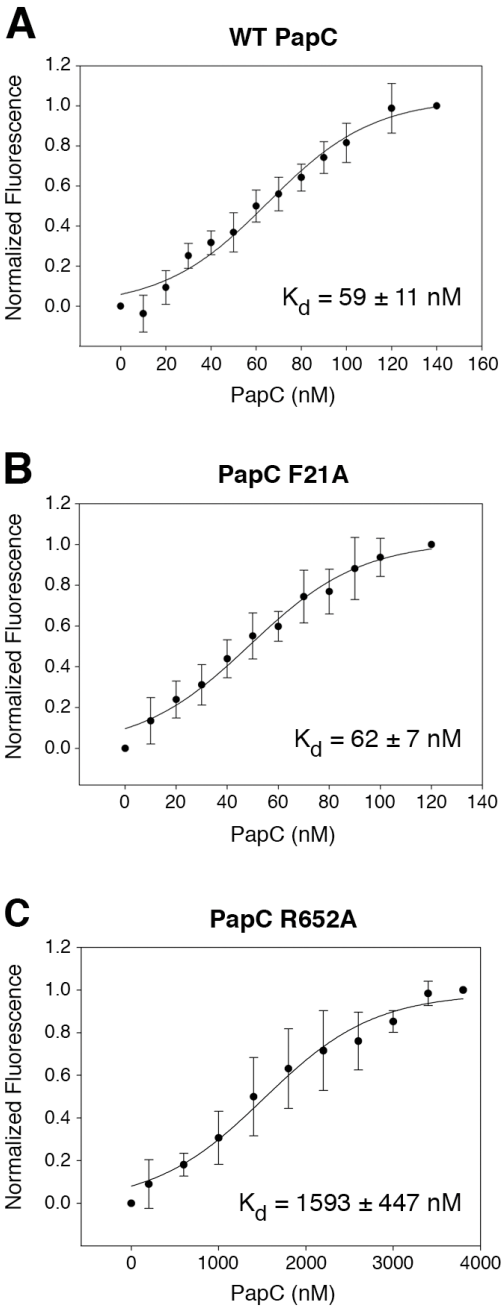

Fig. 4.

Binding affinities of PapC F21A and R652A for PapDG chaperone-adhesin complexes. Fluorescently labeled PapDG was added to cuvettes at 25 nM final concentration. WT PapC (A), PapC F21A (B) or PapC R652A (C) was then titrated into the cuvettes and fluorescence spectra recorded. The graphs represent normalized changes in total fluorescence emission intensity plotted as a function of PapC concentration, where the total changes in intensity ranged from 21 to 34%. The points represent means ± standard deviation of at least three independent experiments, with one-to-three replicates per experiment. Apparent K_d values were obtained by fitting the data to a sigmoidal curve.

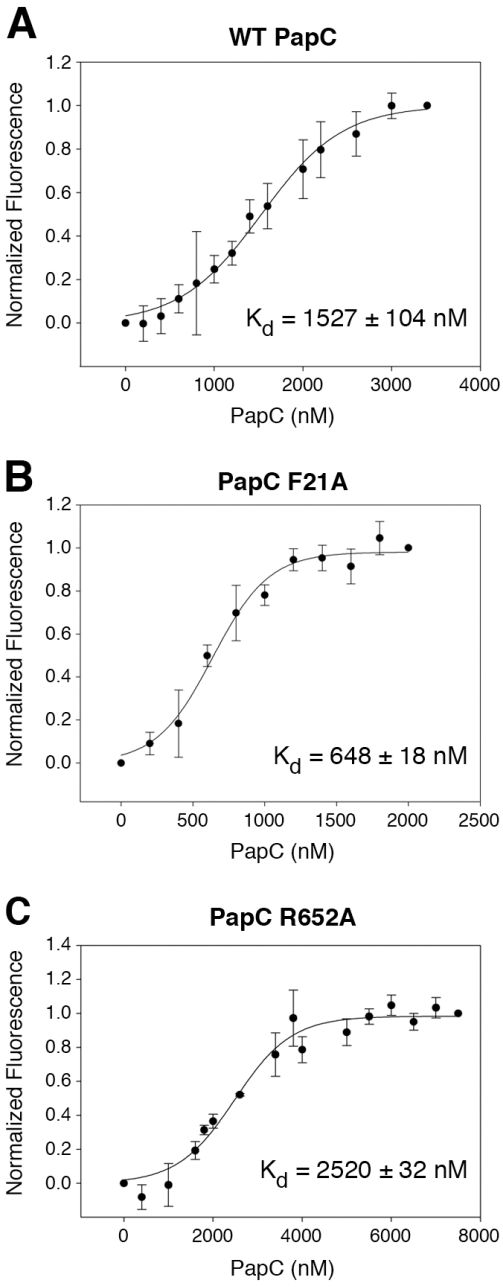

Fig. 5.

Binding affinities of PapC F21A and R652A for PapDA chaperone-rod subunit complexes. Fluorescently labeled $PapDA_{nteK}$ was added to cuvettes at 25 nM final concentration. WT PapC (A), PapC F21A (B) or PapC R652A (C) was then titrated into the cuvettes and fluorescence spectra recorded. The graphs represent normalized changes in total fluorescence emission intensity plotted as a function of PapC concentration, where the total changes in intensity ranged from 16 to 72%. The points represent means ± standard deviation of at least three independent experiments, with one-to-three replicates per experiment. Apparent K_d values were obtained by fitting the data to a sigmoidal curve.

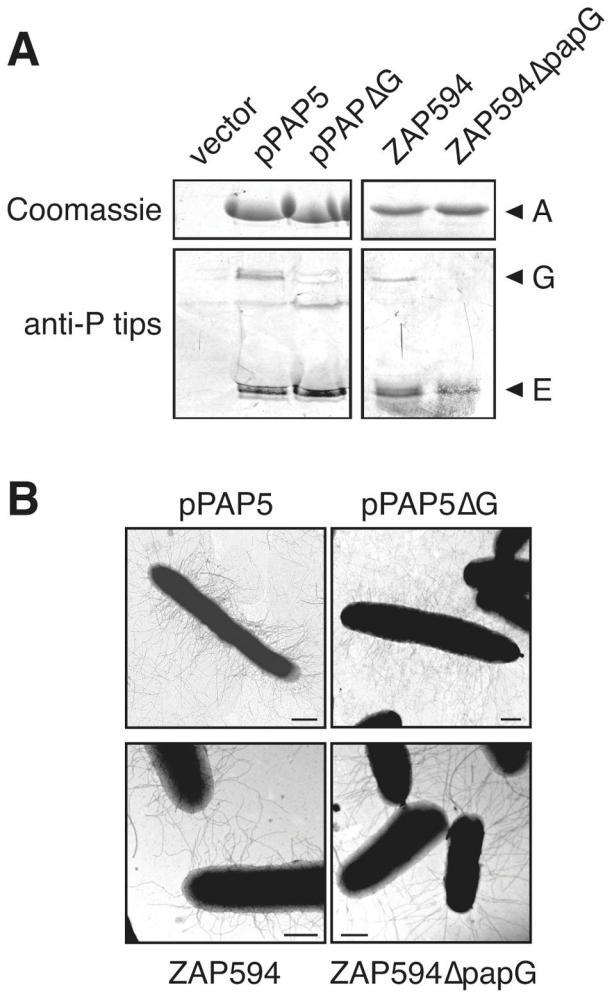

Fig. 6.

PapG is not required for P pilus assembly.

A. Pilus purification. Pili were isolated by heat extraction and magnesium precipitation from the surface of strains AAEC185/pBR322 (vector control), AAEC185/pPAP5 (WT *pap* gene cluster), AAEC185/pPAPΔG (Δ*papG pap* gene cluster), ZAP594/pHGM98 (chromosomal *pap* gene cluster with plasmid-encoded *papI* regulator) and ZAP594ΔpapG/pHGM98 (chromosomal Δ*papG pap* gene cluster with plasmid-encoded *papI* regulator). The pilus preparations were subjected to SDS-PAGE and the PapA major rod subunit (A, upper panel) was visualized by Coomassie blue staining. Pilus tip subunits (PapG and E, lower panel) were detected by immunoblotting with anti-P pilus tips antiserum.

B. Strains AAEC185/pPAP5, AAEC185/pPAPΔG, ZAP594/pHGM98 and ZAP594ΔpapG/pHGM98 were examined by whole-bacteria, negative-stain transmission electron microscopy. Scale bars = 500 nm.

Table 1

Assembly of complete pili and pilus tips by PapC F18A and F21A.

PapC	HA titer[a] – pili (PapAHDJKEFG)	HA titer[a] – tips (PapDJKEFG)
vector	0	0
WT	64	256
Δ2-11	0	0
F18A	32	256
F21A	0	128

[a] HA titer is the highest fold dilution of bacteria able to agglutinate human red blood cells.

Table 2

Sensitivity of PapC F21A and R652A to increasing amounts of PapDA.

	HA titer[a] – PapDA expression under arabinose control			
	Arabinose added:			
PapC	0%	0.05%	0.1%	0.5%
vector	0	0	0	0
WT	256	256	256	256
F21A	128	64	4	ND[b]
R652A	128	64	16	8

[a] HA titer is the highest fold dilution of bacteria able to agglutinate human red blood cells.

[b] ND, not determined.

Table 3

Strains and plasmids used in this study.

Strain or plasmid	Relevant characteristic(s)	Reference or source
Strains[a]		
Tuner	OmpT$^-$ Lon$^-$	Novagen
DH5α	*hsdR recA endA*	(Grant *et al.*, 1990)
SF100	Δ*ompT*	(Baneyx and Georgiou, 1990)
AAEC185	Δ*fim*	(Blomfield *et al.*, 1991)
C600	F-*thr leu thi lac tonA*	(Campbell, 1961)
ZAP594	J96 *pap* gene cluster integrated into chromosome of MG1655	(Holden *et al.*, 2007)
ZAP594ΔpapG	ZAP594Δ*papG*	This study
Plasmids		
pMON6235Δcat	vector, P_{ara}, Amp^r	(Jones *et al.*, 1997)
pACYC184	vector, Tet^r and Clm^r	(Rose, 1988)
pBR322	vector, Tet^r and Amp^r	(Watson, 1988)
pMJ2	Δ*papC pap* operon in pACYC184, P_{trc}, Tet^r	(Thanassi *et al.*, 1998)
pPAP58	PapDJKEFG in vector pMMB91, P_{tac}, Kan^r	(Hultgren *et al.*, 1989)
pMJ3	PapC with C-terminal His-tag in pMON6235Δcat	(Thanassi *et al.*, 1998)
pDG2	pMJ3 with thrombin cleavage site before His-tag	(Li *et al.*, 2004)
pDGT10	PapC in pACYC184, P_{trc}, Tet^r	This study
pAP3	PapC Δ2-11 in pMJ3	(Ng *et al.*, 2004)
pTN35	pAP3 with thrombin cleavage site before His-tag	This study
pTN51	PapC F18A in pMJ3	This study
pTN52	PapC F21A in pMJ3	This study
pSS21	PapC R652A in pMJ3	(Shu Kin So and Thanassi, 2006)
pQY21	pTN52 with thrombin cleavage site before His-tag	This study
pQY652	pSS21 with thrombin cleavage site before His-tag	This study
pSSF21A	PapC F21A in pDGT10	This study
pSSR652A	PapC R652A in pDGT10	This study
pDF1	PapD with His-tag in vector pMMB91, P_{tac}, Kan^r	(Sauer *et al.*, 2002)
pNH200	PapD with thrombin cleavage site and His-tag in pMON6235Δcat	This study
pPAPDA	PapDA in vector pBAD18-cm, P_{ara}, Clm^r	This study
pJP1	PapDG (class I) in vector pMMB91, P_{tac}, Kan^r	(Dodson *et al.*, 1993)
pTN17	PapG (class II) in vector pMMB66, P_{tac}, Amp^r	This study
pTRYC-K1A	PapA with PapK Nte in pACYC184, P_{trc}, Clm^r	This study
pPAP5	J96 *pap* gene cluster in vector pBR322	(Lindberg *et al.*, 1984)
pPAPΔG	Δ*papG pap* gene cluster in pPAP5	This study
pHGM98	pACYC184 with inducible papI, Tet^r	(Holden *et al.*, 2007)

[a] All strains are *E. coli* K-12, except Tuner, which is *E. coli* B.

Amp^r, ampicllin resistance; Kan^r, kanamycin resistance; Clm^r, chloramphenicol resistance; Tet^r, tetracycline resistance; P$_{ara}$, arabinose-inducible promoter, P$_{tac}$ or P$_{trc}$, IPTG-inducible promoter.